The ISME Journal (2021) 15:2627–2642
https://doi.org/10.1038/s41396-021-00956-4

ARTICLE

Regulation of olfactomedin 4 by *Porphyromonas gingivalis* in a community context

Zackary R. Fitzsimonds[1] · Chengcheng Liu[1,5] · Kendall S. Stocke[1] · Lan Yakoumatos[1] · Brian Shumway[2] · Daniel P. Miller[3] · Maxim N. Artyomov[4] · Juhi Bagaitkar[1] · Richard J. Lamont[1]

Received: 21 October 2020 / Revised: 23 February 2021 / Accepted: 1 March 2021 / Published online: 17 March 2021

Abstract

At mucosal barriers, the virulence of microbial communities reflects the outcome of both dysbiotic and eubiotic interactions with the host, with commensal species mitigating or potentiating the action of pathogens. We examined epithelial responses to the oral pathogen *Porphyromonas gingivalis* as a monoinfection and in association with a community partner, *Streptococcus gordonii*. RNA-Seq of oral epithelial cells showed that the Notch signaling pathway, including the downstream effector olfactomedin 4 (OLFM4), was differentially regulated by *P. gingivalis* alone; however, regulation was overridden by *S. gordonii*. OLFM4 was required for epithelial cell migratory, proliferative and inflammatory responses to *P. gingivalis*. Activation of Notch signaling was induced through increased expression of the Notch1 receptor and the Jagged1 (Jag1) agonist. In addition, Jag1 was released in response to *P. gingivalis*, leading to paracrine activation. Following Jag1-Notch1 engagement, the Notch1 extracellular domain was cleaved by *P. gingivalis* gingipain proteases. Antagonism by *S. gordonii* involved inhibition of gingipain activity by secreted hydrogen peroxide. The results establish a novel mechanism by which *P. gingivalis* modulates epithelial cell function which is dependent on community context. These interrelationships have relevance for innate inflammatory responses and epithelial cell fate decisions in oral health and disease.

Introduction

Oral epithelial cells are central to the maintenance of homeostasis in the face of a diverse and abundant microbiota. In addition to constituting a physical barrier, epithelial cells are among the first host cells to recognize oral bacteria and respond with a tailored immune program which in health constrains microbial overgrowth and limits inflammatory tissue damage. The interface of the epithelium with oral bacterial communities is foundational to the pathogenesis of periodontitis, and may also contribute to oral squamous cell carcinoma (OSCC) [1–3]. Pathogenic, or nososymbiotic, communities are populated by large numbers of organisms considered commensals in an individual context [1, 4, 5]. A major unanswered question, therefore, is the extent to which organisms that are commensal can potentiate or mitigate virulence when in combination with pathogens.

Recent studies have begun to shed light on the complexity of the interactions between traditional commensals such as *Streptococcus gordonii*, and pathogens such as *Porphyromonas gingivalis*. In the context of periodontitis, *S. gordonii* acts as an accessory pathogen, inducing an increase

Supplementary information The online version contains supplementary material available at https://doi.org/10.1038/s41396-021-00956-4.

✉ Richard J. Lamont
rich.lamont@louisville.edu

[1] Department of Oral Immunology and Infectious Diseases, University of Louisville School of Dentistry, Louisville, KY 40202, USA

[2] Department of Diagnosis and Oral Health, University of Louisville School of Dentistry, Louisville, KY 40202, USA

[3] Department of Microbiology and Immunology, Virginia Commonwealth University, Richmond, VA 23298, USA

[4] Department of Pathology and Immunology, Washington University School of Medicine, 660S Euclid Avenue, St. Louis, MO 63110, USA

[5] Present address: State Key Laboratory of Oral Diseases, National Clinical Research Center for Oral Diseases, West China Hospital of Stomatology, Sichuan University, Chengdu, 610041 Sichuan, China

in adhesin expression in *P. gingivalis*, and elevating pathogenicity in animal models of alveolar bone destruction [6–8]. In contrast, at the epithelial interface, *S. gordonii* can act as a homeostatic commensal, diminishing the dysbiotic influence of *P. gingivalis* through intercepting host cell signaling pathways [9]. For example, as a monoinfection of gingival epithelial cells, *P. gingivalis* can activate FOXO1 signaling which increases expression of ZEB2 and initiates an epithelial mesenchymal transition (EMT). However, in dual species infection, *S. gordonii* can override this signaling program by activating the TAK1-NLK negative regulatory pathway which represses FOXO1, thus preventing ZEB2 upregulation and maintaining eubiosis [10].

P. gingivalis can impinge upon multiple signaling pathways in epithelial cells, resulting in changes in tissue and immune homeostasis, all of which could potentially be modulated by oral streptococci [2, 11, 12]. In this study we undertook a comprehensive analysis of the gingival epithelial cell pathways regulated in response to *P. gingivalis* alone, but which are overridden by *S. gordonii*. Transcriptional profiling identified the Notch pathway in this category, and the downstream target of Notch signaling, olfactomedin 4 (OLFM4), was a key component of epithelial cell migratory, proliferative and inflammatory responses to *P. gingivalis* which could be suppressed by *S. gordonii*. These results establish both a novel signaling axis by which *P. gingivalis* modulates epithelial cell function, along with a new mechanism for microbial interplay in the community context which provides a molecular underpinning of both polymicrobial synergy and antagonism.

Materials and methods

Bacterial strains, eukaryotic cells, antibodies, and reagents

Bacterial strains are listed in Supplementary Table S1. Bacteria were cultured anaerobically unless otherwise noted. *P. gingivalis* strain 33277 was used in all experiments unless otherwise indicated. Eukaryotic cells are listed in Supplementary Table S2. Cells were grown to ~80% confluence and challenged with bacteria at a multiplicity of infection (MOI) of 100 for 1 h, followed by 23 h in fresh medium, unless otherwise noted. For co-infections, bacteria were added for a total MOI of 100, unless otherwise indicated. Antibodies, siRNA, and reagents are listed in supplementary Table S3.

RNAseq

RNA was extracted using the RNAqueous-Micro Total RNA Isolation kit (ThermoFisher, Waltham, MA). The TruSeq Stranded Total RNA with RiboZero Plus kit (Illumina, San Diego, CA) was used to generate a sequencing library from 1 µg of total RNA. Paired-end sequencing was performed on an Illumina Nextseq 500 at the University of Louisville Genomics Core using the Nextseq 500 High-Output Kit (150 cycles). Base calls used the BaseSpace FastQ Version 1.0.0 application (Illumina). Raw gene counts with a minimum of two counts per million in at least one sample were used for downstream analyses. Differentially expressed genes were determined by the DESeq2 Bioconductor/R package (https://doi.org/10.18129/B9.bioc.DESeq2), and *p* values were adjusted for multiple comparisons using the Benjamini-Hochberg procedure [13]. Cutoffs of 1 for the log2 fold change and an adjusted *p* value of 0.05 were considered significant. Volcano plots were generated with the EnhancedVolcano Bioconductor/R package (DOI: 10.18129/B9.bioc.EnhancedVolcano), and functional enrichment analysis was performed with the String Database version 11 [14] using an FDR stringency of 1 percent and a minimum interaction confidence score of 0.400 for network generation. For principal component analysis (PCA) and heatmap generation, the raw count data were made homoscedastic using a regularized logarithm [15]. PCA was conducted using base R [16] and PCA plots generated using the ggfortify R package [17]. Gene counts for heatmap generation were converted into z-scores and input into the ComplexHeatmap Bioconductor/R package [18]. Visualization of sets of differentially expressed genes in common amongst treatment groups was performed using the ComplexUpset R package based on the UpSet plot technique [19] for multiple set comparison. All sequencing reads were deposited in the Gene Expression Omnibus (GEO), # GSE159868.

Quantitative (q) reverse transcription (RT)-PCR

RNA was purified using an RNAeasy plus kit (Qiagen, Germantown, MD). 2 µg RNA were reverse transcribed using a high capacity reverse transcription kit (Thermofisher). Applied Biosystems Taqman fast universal master mix and Taqman gene expression assays were from Thermofisher. qRT-PCR cycle threshold (Ct) values were normalized to GAPDH, and fold changes were calculated using 2-ΔΔCT.

Plasmid preparation, RNA interference, transfections, and luciferase assay

The OLFM4 promoter-luciferase reporter construct was made by amplification of a 500 bp fragment upstream of the *OLFM4* coding sequence, which was cloned into pGL3-basic plasmid (Promega, Madison, WI). All constructs were confirmed by sequencing. The internal control reporter was

pRL vector which provides constitutive expression of Renilla luciferase (Promega). For siRNA (Supplementary Table S3), cells were grown to 50-60% confluence, and cells for plasmid transfection were grown to 60–70% confluence. Transfection was for 48 h using Lipojet (SignaGen, Gaithersburg, MD), and medium was replaced for 24 h before bacterial challenge. Confirmations of knockdowns is in Supplementary Fig. S1. Luciferase reporter assays were performed using a Stop & Glo Dual luciferase reporter kit (Promega). Luciferase activity was measured using a 10 s integration time in a Luminometer (Molecular Devices, San Jose, CA), and normalized to Renilla luciferase activity from the same lysates.

Immunofluorescence and confocal laser scanning microscopy

Telomerase Immortalized Gingival Keratinocytes (TIGKs) were challenged with bacteria then fixed, permeabilized and probed with primary antibodies, Alexa Fluor 488-labeled secondary antibodies, Texas Red-phalloidin, and DAPI as described [10]. Slides were scanned with a Leica SP8 confocal microscope, and images were analyzed with Volocity 6.3 Software (PerkinElmer, Waltham MA). Nuclear localization was quantified using the 3D image processing software IMARIS (Bitplane AG, Concord, MA). The Surfaces function in Imaris was used to create a 3D model of the nuclei from the DAPI channel, and then calculate Alexa Fluor 488 voxels within each nucleus, which was normalized to the volume of the nucleus. Total normalized Alexa Fluor 488 was divided by the number of cells analyzed.

Immunoblots and ELISA

Cells were lysed using RIPA buffer containing Protease and PhosSTOP phosphatase inhibitor (Roche, Indianapolis, IN). Proteins (20 µg) were separated by 10% SDS-PAGE, and immunoblotted as described [10]. For ELISA, cell culture supernatant was centrifuged for 20 min at 20,000 × *g* at 4 °C, filtered (0.4 µm) and concentrated using Amicon (Temecula, CA) Ultra concentrators. Supernatant (25 µl) was used per manufacturer's guidelines: R&D Systems (Minneapolis, MN) for CXCL10/IP-10, and LifeSpan BioSciences (Seattle, WA) for OLFM4. Amounts reported are prior to concentration.

Transwell assays

For bacterial interactions with TIGKs, cells were grown only in the lower chamber of a 0.4 µm transwell filter plate (Millipre Sigma, St. Louis, MO). Cells were challenged with *P. gingivalis*, and the upper chamber contained streptococcal strains. For studying epithelial cell-to-cell interactions, TIGKs were cultured in both the lower chamber and on the transwell insert in the upper chamber. *P. gingivalis* was added to the upper chamber only.

To measure TIGK migration, cells (2×10^5) were seeded onto the matrigel insert in the upper chamber, and cultured for 18 h. Cells migrating through the filter were fixed with 1% methanol, and stained with Diff-quick stain (AmScope, Irvine, CA). Cells were counted from three random fields at 20× using a Nikon Eclipse T100 microscope.

Proliferation and apoptosis assays

TIGKs were labeled with BrdU 2 h prior to the end of the infection period, and BrdU measured with a Cell Proliferation ELISA kit (Abcam, Cambridge, MA) according to the manufacturer's protocol. To measure apoptosis, TIGKs were challenged with *P. gingivalis* and treated with camptothecin (CAM) at 1 µg/mL for 4 h. Apoptosis was determined by detection of caspase-3 activity on a fluorescent substrate (EnzChek, Carlsbad, CA).

Gingipain activity

Gingipain activity was determined as previously described [7] using the chromogenic substrate L-BAPNA. The rate of accumulation of p-nitroanilide was monitored spectrophotometrically at 405 nm over time in a Spectramax M5 reader (Molecular Devices).

Statistical analysis

Assays were performed with at least three biological replicates. Confocal images are representative of three biological replicates with at least three randomly scanned areas of the chamberslide. ANOVA with Tukey's multiple comparison test were conducted using GraphPad Prism V8. Statistical analyses of RNA-Seq data are described above.

Results

Epithelial responses to *P. gingivalis* alone and in dual species conglomerates with *S. gordonii*

RNA-Seq was used to reveal the transcriptional profile of TIGKs induced by *P. gingivalis* 33277, but normalized or reversed by *S. gordonii* DL1. PCA analysis (Supplementary Fig. S2A) showed tight clustering of samples within the same group and separation between each of the groups, indicating distinct transcriptional responses. UpSet charts (Supplementary Fig. S2B, C) established that antagonism of *P. gingivalis* by *S. gordonii* is broadly based, as the transcriptional profile of the combined *P. gingivalis* + *S. gordonii* group (PgSg) more closely resembles the *S. gordonii* (Sg) only group than

it does the *P. gingivalis* (Pg) only group. The percentage of differentially regulated genes in the PgSg vs. the no infection (NI) condition that is shared with the Sg vs. NI condition is over 8-fold higher than the amount shared with the Pg vs. NI condition. Volcano plots (Supplementary Fig. S2D–G) and a heat map analysis (Fig. 1A) showed that genes involved in Notch signaling were enriched in response to *P. gingivalis* and trended toward homeostasis in the presence of *S. gordonii*. Of the Notch-regulated genes, *OLFM4* showed the greatest change between the *P. gingivalis* alone condition (134-fold upregulated) and the PgSg condition (59-fold downregulated). OLFM4 is an antiapoptotic glycoprotein which promotes tumor growth [20], and is selectively expressed in inflamed epithelium [21], suggesting an important role in the oral cavity.

qRT-PCR confirmed the upregulation of *OLFM4* by *P. gingivalis* in a time and dose dependent manner, with an over 2000-fold increase in mRNA after 48 h at an MOI of 100 (Fig. 1B). However, as OLFM4 is secreted, in order to focus on direct effects of *P. gingivalis*, subsequent experiments utilized a 24 h incubation period. An increase in OLFM4 protein levels in response to *P. gingivalis* was corroborated by western blotting, ELISA and confocal microscopy (Fig. 1C–E). To confirm that regulation of *OLFM4* mRNA tracked with an increase in promoter activity, TIGKs were transfected with a luciferase-reporter construct containing the *OLFM4* upstream regulatory sequences [20]. After challenge with *P. gingivalis*, *OLFM4* promoter activity increased at 6 h through 24 h (Fig. 1F). We explored multiple *P. gingivalis* strains to verify upregulation of *OLFM4* is a property conserved across the species. Fig. 1G shows all tested strains induced elevated *OLFM4* expression, including the fimbriated/non-encapsulated lineage (33277, 381), the encapsulated/afimbrial lineage (W83), the fimbriated/encapsulated lineage (A7A1-28) and the low-passage clinical isolate MP4-504 [22–25]. Next, we determined whether *OLFM4* regulation by *P. gingivalis* is specific to gingival epithelial cells. *OLFM4* was upregulated in the OKF6 line, which are telomerase immortalized buccal mucosa cells, albeit to lower levels than occur in TIGKs (Fig. 1H). Tongue (SCC9) and esophageal (ESCC9706) squamous cell carcinoma cells also displayed a modest increase in *OLFM4* mRNA expression (Fig. 1H). These results indicate that epithelial cells of the gingiva, which is the primary in vivo habitat of *P. gingivalis*, are more responsive to challenge with the organism, at least in terms of *OLFM4* regulation, as compared to cells derived from other sites in the oral and esophageal regions.

Role of OLFM4 in prosurvival phenotypes of TIGKs

OLFM4 has been shown to promote the proliferation and migration of cells in culture [26, 27], and consistent with this, siRNA-knockdown of OLFM4 suppressed TIGK proliferation and migration into matrigel in response to *P. gingivalis* (Fig. 2A, B). OLFM4 can also contribute to apoptosis resistance [28, 29], however, knockdown of OLFM4 had no effect of *P. gingivalis* antagonism of camptothecin-induced apoptosis (Supplementary Fig. S3). Taken together, these results show that the dramatic increase in OLFM4 is significant in controlling epithelial cell proliferation and migration responses to *P. gingivalis*, while apoptosis resistance is mediated by an independent pathway.

Jag1-Notch1 signaling is required for OLFM4 regulation by *P. gingivalis*

To explore the mechanism of Notch-dependent signaling in OLFM4 regulation, we first verified and extended the nature of the impact of *P. gingivalis* challenge on Notch receptor and ligand mRNA expression using qRT-PCR. Fig. 3A shows that the Notch1 and Notch3 receptors are upregulated in response to challenge with *P. gingivalis*. siRNA knockdown of Notch 1–4 showed that a reduction in Notch1 decreased OLFM4 mRNA levels in *P. gingivalis* challenged cells (Fig. 3B). Knockdown of Notch 2 and 4 had no effect on OLFM4 expression, whereas knockdown of Notch3 significantly increased levels of OLFM4 mRNA, possibly due to increased availability or expression of Notch1.

Notch signaling is activated by the ligands Jagged (Jag)1, Jag2, DLL1, DLL3 and DLL4, and qRT-PCR revealed that *P. gingivalis* upregulated expression of Jag1, while Jag2 was downregulated (Fig. 3C), consistent with the RNA-Seq data. siRNA knockdown of Jag1 led to decreased induction of OLFM4 by *P. gingivalis*, whereas suppression of DLL 1, 3, or 4 did not influence OLFM4 mRNA levels (Fig. 3D). Knockdown of Jag2 increased OLFM4 transcription, indicating that Jag2 expression may interfere with signaling through Notch1. A reduction in Notch1 and Jag1 also diminished *P. gingivalis*-dependent regulation of an additional target of the Notch signaling pathway, Hes5 (Fig. 3E), corroborating the importance of Jag1-Notch1 signaling in TIGK responses to the organism.

In addition to canonical cell-cell Jag1-Notch1 activation, it was recently established that endothelial cells can cleave and release a soluble form of Jag1 which then binds and activates Notch receptors on colorectal cancer cells [30]. To explore whether a similar mechanism of paracrine activation occurs in our model, we utilized a transwell system. When cells in the upper chamber were challenged with *P. gingivalis*, *OLFM4* transcription was induced in the lower chamber cells, and this effect was lost when Jag1 was suppressed in the upper chamber cells (Fig. 3F).

OLFM4 is also a target gene of the Wnt/β-catenin pathway [21] which can be activated by *P. gingivalis* [31];

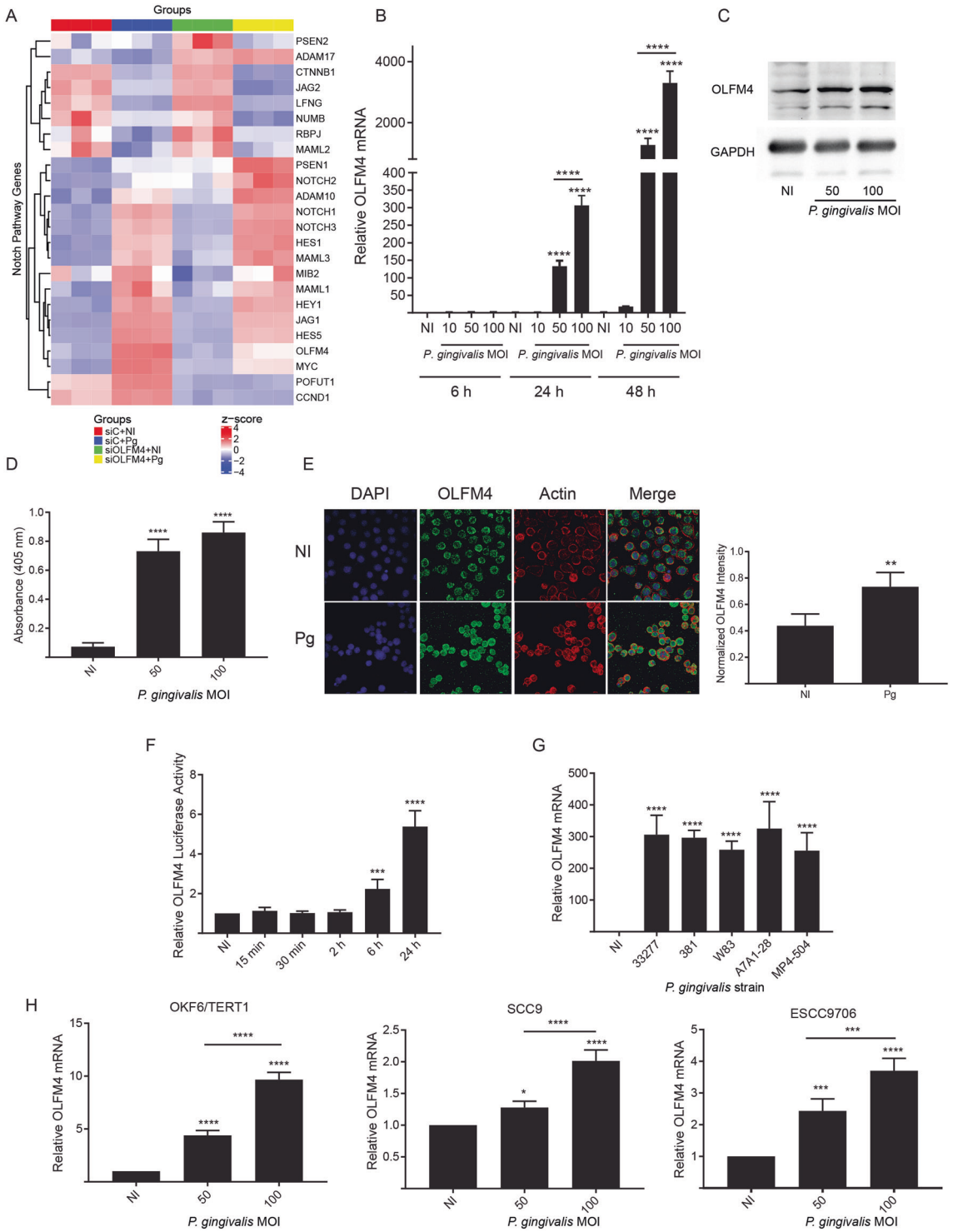

however, neither pharmacological inhibition of Wnt nor siRNA knockdown of β-catenin affected OLFM4 induction in response to *P. gingivalis* (Supplementary Fig. S4A, B). *In silico* interrogation of the promoter region of *OLFM4* revealed the presence of a ZEB2 consensus binding element. ZEB2 activity is enhanced by *P. gingivalis* and antagonized by *S. gordonii;* however, siRNA knockdown of ZEB2 did not prevent increased OLFM4 mRNA production in response to *P. gingivalis* (Supplementary Fig. S4C). Collectively, these results indicate that OLFM4 regulation by *P. gingivalis* occurs through increased transcriptional activity of the *NOTCH1* and *JAG1* genes, along with release of soluble Jag1 and activation of the Notch1 pathway on adjacent cells.

◀ **Fig. 1 Responses of TIGKs to *P. gingivalis* involve the Notch signaling pathway and OLFM4. A** Hierarchical clustering heatmap, based on RNA-Seq log (RPKM) values, of Notch pathway genes differentially regulated by *P. gingivalis* (Pg) and/or *S. gordonii* (Sg) challenge in TIGKs. Color intensity denotes level of gene expression by z-score. **B** qRT-PCR of TIGK cells infected with *P. gingivalis* at the times and MOIs indicated. OLFM4 mRNA levels are expressed relative to noninfected (NI) controls. **C** Immunoblot of lysates of TIGK cells challenged with *P. gingivalis* at MOI 50 or 100 for 24 h, and probed with OLFM4 antibodies or GAPDH antibodies as a loading control. **D** ELISA of OLFM4 in supernatants of TIGKs challenged with *P. gingivalis* at indicated MOIs for 24 h. **E** Fluorescent confocal microscopy of TIGK cells infected with *P. gingivalis* at MOI 100 for 24 h (Pg) or noninfected (NI). Cells were probed with OLFM4 antibodies and Alexa Fluor 488 secondary antibodies (green). Actin (red) was stained with Texas Red-phalloidin, and nuclei (blue) stained with DAPI. Cells were imaged at magnification ×63, and shown are projections of z-stacks. OLFM4 staining intensity was normalized to DAPI staining and quantified in over 200 cells with Volocity software. **F** TIGKs were transiently transfected with an OLFM4 promoter–luciferase reporter plasmid, or a constitutively expressing Renilla luciferase reporter. Cells were challenged with *P. gingivalis* MOI 100 for the times indicated. NI is no infection control. OLFM4 luciferase activity was normalized to the level of Renilla luciferase. **G** qRT-PCR, as in **B**, of OLFM4 mRNA levels in TIGKs challenged with the *P. gingivalis* strains indicated, or left uninfected (NI). **H** qRT-PCR, as in **B**, of OLFM4 mRNA levels in the cell types indicated following *P. gingivalis* challenge. Quantitative data are means with SEM. $*p < 0.05$, $**p < 0.01$, $***p < 0.005$, $****p < 0.001$ compared to NI unless indicated. Images are representative of three independent experiments.

P. gingivalis gingipains activate Notch signaling

To identify effector molecules of *P. gingivalis* responsible for activating Notch signaling, we examined a panel of mutants in established virulence or colonization factors. As shown in Fig. 4A, loss of fimbrial adhesins or of serine and tyrosine phosphatases did not impact the ability of *P. gingivalis* to regulate OLFM4. In contrast, the Δ*rgpAB*Δ*kgp* mutant, which is deficient in the production of the arginine specific (RgpA and RgpB) and lysine specific (Kgp) gingipain proteases, was unable to stimulate OLFM4 production. Gingipains are secreted through the type IX secretion system (T9SS), and loss of PorK, which is required for formation of a functional secretion pore [32], also abrogated the ability of *P. gingivalis* to enhance *OLFM4* transcription. We further investigated the role of gingipains by challenging cells with individual gingipain mutants, which revealed that loss of either Kgp or RgpA/B was sufficient to prevent upregulation of OLFM4 (Fig. 4B). In addition, pretreatment of parental *P. gingivalis* with the gingipain inhibitor TLCK diminished OLFM4 responses.

Engagement of the Notch receptor by Jag1 induces a conformational change in the Notch protein which exposes an extracellular region that can be cleaved by the extracellular proteases ADAM10 and ADAM17 [33]. On the basis of the results with gingipains, we hypothesized that

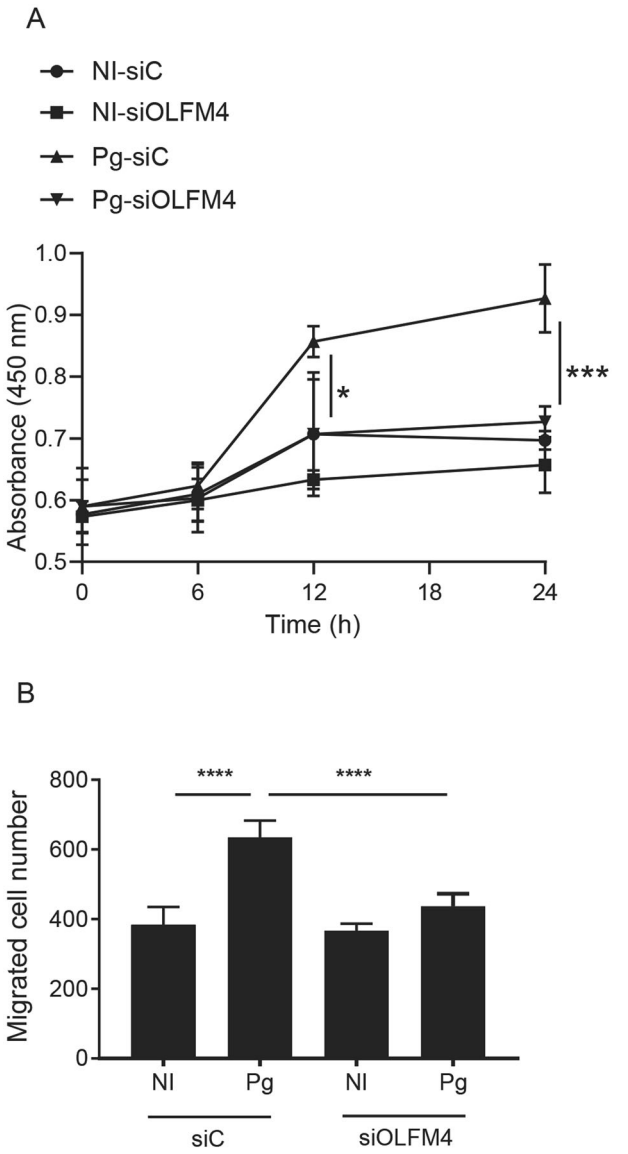

Fig. 2 OLFM4 is required for proliferation and migration induced by *P. gingivalis* in TIGKs. A BrdU proliferation ELISA of TIGKs transiently transfected with siRNA to OLFM4 or scrambled siRNA (siC), and infected with *P. gingivalis* (Pg) or left uninfected (NI). Absorbance at 450 nm was measured over the times indicated. **B** Quantitative analysis of TIGK migration through matrigel-coated transwells. TIGK cells were transiently transfected with siRNA to OLFM4 or scrambled siRNA (siC), and infected with *P. gingivalis* (Pg) or left uninfected (NI). Data are the mean with SD number of cells invading through inserts coated with Matrigel, and are representative of three biological replicates. $*p < 0.05$, $***p < 0.005$, $****p < 0.001$.

these proteolytic enzymes of *P. gingivalis* activate signaling through cleavage of the extracellular domain of Notch. As shown in Fig. 4C, *P. gingivalis* remained capable of activating Notch in the presence of TAPI-2, suggesting that the gingipains can functionally compensate for the loss of the ADAM10 and ADAM17. This was corroborated by siRNA targeting ADAM10 and ADAM17, which also failed to

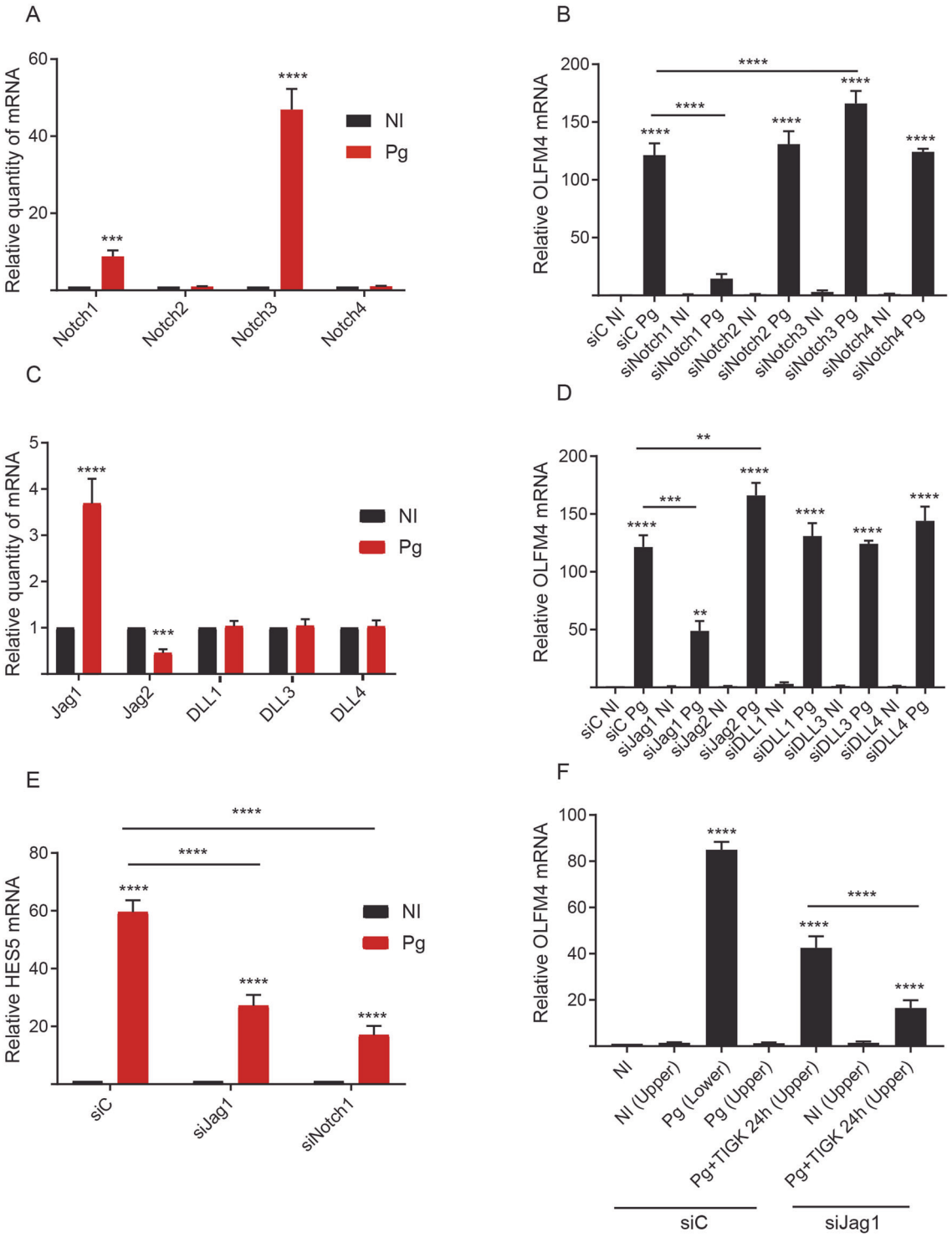

prevent activation of Notch and upregulation of OLFM4 (Fig. 4D). In contrast, DAPT, which is an inhibitor of γ-secretase, the enzyme that cleaves the intracellular domain of the Notch receptors, completely inhibited stimulation of *OLFM4* transcription by *P. gingivalis* (Fig. 4E). Thus, the gingipains are unable to complement cleavage of the intracellular domain of Notch, and function extracellularly to activate Notch.

Overall, we conclude that *P. gingivalis* increases expression of the Notch1 receptor and its Jag1 ligand, and receptor signaling is then amplified by cleavage of the Notch1 extracellular domain by gingipain proteases. In a

◀ **Fig. 3 Regulation of Notch signaling by *P. gingivalis*.** **A** TIGK cells were infected with *P. gingivalis* (Pg) and expression of Notch receptor mRNA was measured by qRT-PCR. Data are expressed relative to noninfected (NI) controls. **B** TIGK cells were transiently transfected with siRNA to Notch receptors or scrambled siRNA (siC) and infected with *P. gingivalis* (Pg). OLFM4 mRNA levels were measured by qRT-PCR. Data are expressed relative to noninfected (NI) controls. **C** TIGK cells were infected with *P. gingivalis* (Pg) and expression of Notch agonist mRNA was measured by qRT-PCR. Data are expressed relative to noninfected (NI) controls. **D** TIGK cells were transiently transfected with siRNA to Notch agonists or scrambled siRNA (siC) and infected with *P. gingivalis* (Pg). OLFM4 mRNA levels were measured by qRT-PCR. Data are expressed relative to noninfected (NI) controls. **E** TIGK cells were transiently transfected with siRNA to Jag1 or Notch1, or scrambled siRNA (siC) and infected with *P. gingivalis* (Pg). Hes5 mRNA levels were measured by qRT-PCR. Data are expressed relative to noninfected (NI) control. **F** TIGK cells were grown in the lower and upper chambers of transwell plates. Cells in the upper chamber were transiently transfected with siRNA to Jag1 or scrambled siRNA (siC). Cells were challenged with *P. gingivalis* (Pg) in upper or lower chambers as indicated. Expression of OLFM4 mRNA in cells in the lower chamber was measured by qRT-PCR and expressed relative to noninfected (NI) controls. Quantitative data are means with SEM. $^{**}p < 0.01$, $^{***}p < 0.005$, $^{****}p < 0.001$ compared to NI unless indicated.

second hit, *P. gingivalis* causes an increase in secretion of Jag1 and consequent paracrine activation of Notch1.

Regulation of OLFM4 in the community context

The microbial ecosystem of the oral cavity is a complex multispecies community in which *P. gingivalis* interacts with a variety of partner species [34–36]. Hence, we investigated the impact of several community partners of *P. gingivalis* on OLFM4 regulation. *Filifactor alocis*, *Fusobacterium nucleatum*, or *Treponema denticola*, did not impede regulation of *OLFM4* by *P. gingivalis*, indeed these organisms may synergize with *P. gingivalis* in the induction of *OLFM4*, allowing *P. gingivalis* at MOI 50 to regulate OLFM4 to the same degree as *P. gingivalis* alone at MOI 100 (Fig. 5A). While *T. denticola* has been shown to increase gingipain expression [37], the matter requires more thorough investigation. By contrast, *S. gordonii* antagonized *OLFM4* induction by *P. gingivalis*, and in a three species consortium of *P. gingivalis, F. nucleatum* and *S. gordonii*, the antagonistic effect of *S. gordonii* was dominant. Inhibition by *S. gordonii* was evident at a ratio of 1:10 and exhibited a dose-dependence on the amount of streptococcal cells (Fig. 5B). We verified OLFM4 expression changes at the protein level using an ELISA, which showed that co-infection with *S. gordonii* can reduce the amount of secreted OLFM4 (Fig. 5C). To begin to address the mechanism of *S. gordonii* antagonism, we utilized confocal microscopy to determine the localization pattern of cleaved Notch, the intracellular domain which translocates to the nucleus and activates the transcription factor RBP-JK. Fig. 5D shows that *P. gingivalis*-induced nuclear localization of Notch is reduced in the presence of *S. gordonii*. These results suggest that *S. gordonii* prevents *P. gingivalis*-induced upregulation of OLFM4 by blocking activation of Notch signaling.

Streptococcal peroxide inactivates gingipains

S. gordonii is one of several species of oral streptococci with the potential to conglomerate with *P. gingivalis* in vivo. Additional oral streptococcal species were thus tested for antagonistic properties. *S. oralis* and *S. sanguinis* were also capable of inhibiting OLFM4 expression (Fig. 6A), whereas *S. constellatus* and *S. mutans* were ineffective. One phenotypic property of these streptococcal species which tracks with antagonism of *P. gingivalis* is production of hydrogen peroxide as a metabolic by-product [38]. Thus, we first tested whether secreted metabolites were sufficient to inhibit *OLFM4* expression. In a transwell assay, both *S. gordonii*, S. *oralis*, but not *S. mutans*, in the upper chamber were able to inhibit *OLFM4* induction in TIGKs challenged with *P. gingivalis* in the lower chamber (Fig. 6B). To provide evidence of a role for hydrogen peroxide specifically, we utilized a *S. gordonii* pyruvate oxidase mutant (ΔspxB), in which hydrogen peroxide production is reduced by approximately 90% through loss of conversion of pyruvate to acetate and hydrogen peroxide [38, 39]. As shown in Fig. 6C, suppression of OLFM4 was reduced with the Δ*spxB* mutant in a co-infection assay. In contrast, mutants of *S. gordonii* unable to bind (ΔsspA/B) or accumulate (Δcbe) with *P. gingivalis*, retained their inhibitory ability. Similarly, in a transwell assay with *P. gingivalis* in the lower chamber and *S. gordonii* in the upper chamber, the ΔspxB mutant had no impact on induction of OLFM4 mRNA (Fig. 6D). Complementation of the mutation with the *spxB* gene in trans (CΔspxB) restored the antagonistic phenotype. These results strongly implicate secreted hydrogen peroxide as the effector of streptococcal antagonism of *P. gingivalis*-induced OLFM4 regulation.

A reducing environment is required for gingipain activity, in order to maintain the cysteine in the catalytic domain [40], and we hypothesized that oxidation by hydrogen peroxide would impair gingipain function. Gingipain activity was measured in the supernatants of *P. gingivalis* cultures incubated with streptococci either capable or unable to produce hydrogen peroxide (Fig. 6E). Aerobically cultured *S. gordonii* WT and the complemented strain CΔspxB significantly reduced gingipain activity. The ΔspxB mutant was less efficient at reducing activity, although some reduction did occur, probably due to residual hydrogen peroxide production. Proteolytic activity was unaffected by *S. mutans*

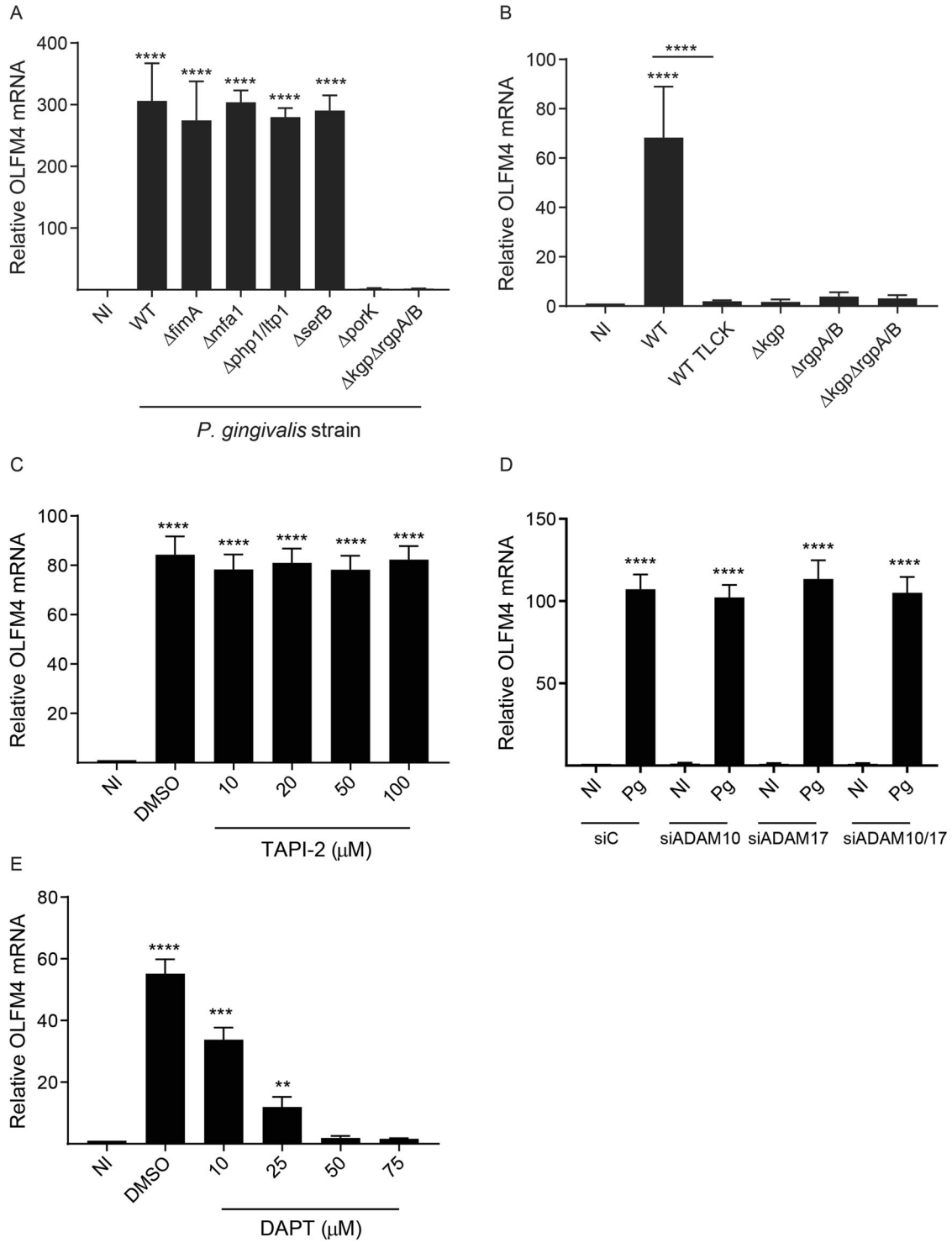

Fig. 4 Activation of Notch signaling by *P. gingivalis* requires gingipains. A, **B** TIGKs were challenged with WT (33277), mutant strains, or WT pretreated with the protease inhibitor TLCK (100 μM, 2 h), and OLFM4 mRNA was measured by qRT-PCR. **C** TIGKs were pretreated with TAPI-2 at the concentrations indicted or DMSO as a vehicle control. Cells were challenged with *P. gingivalis*, and OLFM4 mRNA was measured by qRT-PCR. **D** TIGK cells were transiently transfected with siRNA to ADAM proteases as indicated or scrambled siRNA (siC) and challenged with *P. gingivalis* (Pg). OLFM4 mRNA levels were measured by qRT-PCR. Data are expressed relative to noninfected (NI) controls. **E** TIGK cells were pretreated with DAPT at the concentrations indicted, or DMSO as a vehicle control. Cells were challenged with *P. gingivalis* and OLFM4 mRNA was measured by qRT-PCR. Data are means with SEM $^{**}p < 0.01$, $^{***}p < 0.005$, $^{****}p < 0.001$ compared to NI unless indicated.

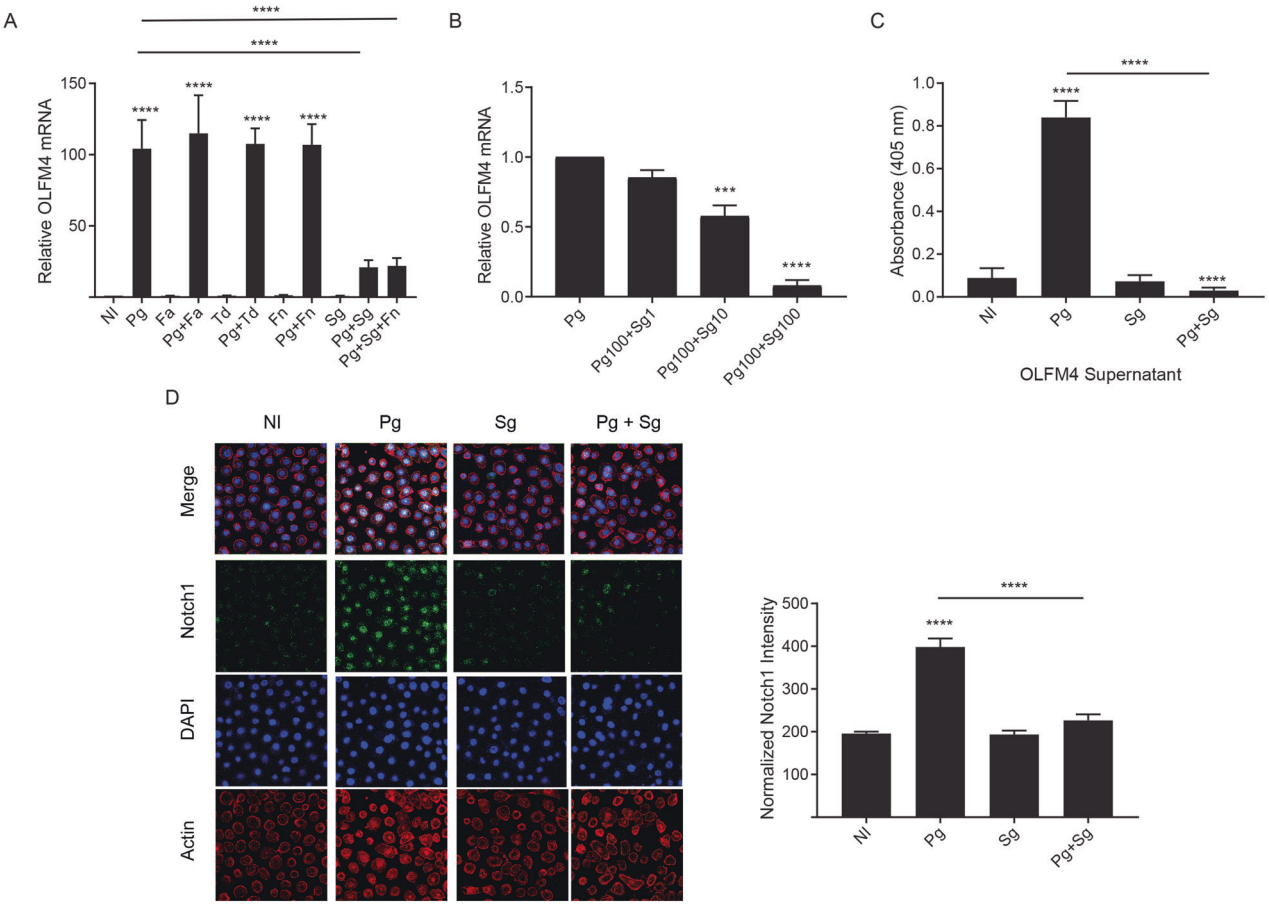

Fig. 5 Impact of community challenge on Notch signaling and OLFM4. A qRT-PCR of OLFM4 mRNA levels in TIGKs either left uninfected (NI) or challenged with *P. gingivalis* (Pg), *F. alocis* (Fa), *T. denticola* (Td), *F. nucleatum* (Fn), or *S. gordonii* (Sg) alone or in equal numbers for a total MOI 100 in the combinations indicated. Data are means with SEM. $^{****}p < 0.001$ compared to NI unless indicated. **B** qRT-PCR of OLFM4 mRNA levels in TIGKs challenged with *P. gingivalis* (Pg) alone MOI 100, Pg MOI 100 and *S. gordonii* (Sg) MOI 1, Pg MOI 100, and Sg MOI 10, or Pg MOI 100 and Sg MOI 100. Data are means with SEM. $^{***}p < 0.005$, $^{****}p < 0.001$ compared to Pg alone. **C** ELISA of OLFM4 in culture supernatant of TIGKs left uninfected (NI), or challenged with Pg or Sg alone or in combination. Data are means with SD and are representative of 3 biological replicates. $^{****}p < 0.001$, compared to NI unless indicated. **D** Fluorescent confocal microscopy of TIGK cells challenged with *P. gingivalis* (Pg) MOI 100, *S. gordonii* (Sg) MOI 100, Pg MOI 50 in combination with Sg MOI 50, or noninfected (NI). Cells were probed with Notch antibodies and Alexa Fluor 488 secondary antibody (green). Actin (red) was stained with Texas Red-phalloidin, and nuclei (blue) stained with DAPI. Cells were imaged at magnification ×63, and shown are projections of z-stacks generated with Volocity. Notch staining intensity localized to the nucleus was normalized to DAPI staining and quantified in over 200 cells with Imaris software. Images are representative of three independent experiments.

and following anaerobic culture of the streptococcal strains, under which conditions hydrogen peroxide is not produced. We then sought to determine the concentrations of hydrogen peroxide that could inhibit gingipain activity. As shown in Fig. 6F, 800 µM was the lowest dose at which significant inhibition of gingipain activity was observed, with greater reduction occurring between 1 and 2 mM, which is the range of hydrogen peroxide levels that can be produced extracellularly by streptococci [41]. These data support the concept that hydrogen peroxide produced by certain species of oral streptococci such as *S. gordonii* inhibit the activity of gingipains and consequently impede activation of the Notch pathway by *P. gingivalis*.

OLFM4 regulates inflammatory responses to *P. gingivalis*

OLFM4 is expressed in inflamed epithelium [42], and is an anti-inflammatory mediator in *Helicobacter pylori* infection [43]. We thus reasoned that OLFM4 may play a role in inflammatory responses to *P. gingivalis* and we performed RNA-Seq on OLFM4 knockdown cells (Supplementary Fig. S5). Gene enrichment analysis (Fig. 7A) showed that expression of a number of immune mediators was suppressed by *P. gingivalis*, consistent with previous studies [44–47], and this effect was lost when OLFM4 was suppressed. We have previously demonstrated antagonism of

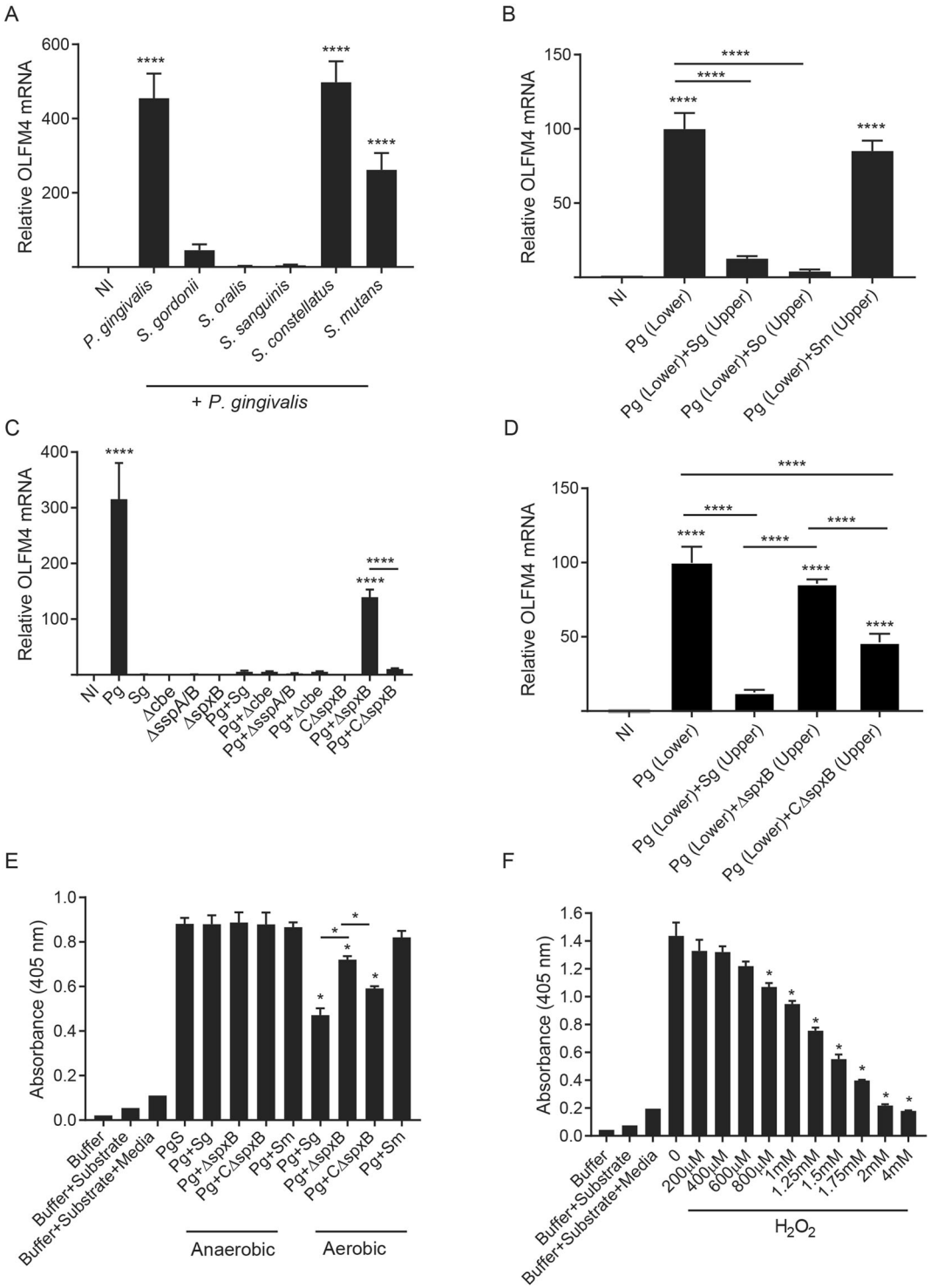

the Th1-biasing cytokine CXCL10 (IP-10) by *P. gingivalis* [44], and qRT-PCR corroborated dependence on OLFM4 (Fig. 7B). ELISA of culture supernatants also showed an increase in CXCL10 protein levels in the siOLFM4 condition, although degradation reduced the amount of CXCL10 following *P. gingivalis* challenge (Fig. 7C).

Discussion

In this study, we identify OLFM4 as significantly regulated in response to a single species challenge with *P. gingivalis*. In the context of a dual-species challenge, however, OLFM4 regulation was overridden by *S. gordonii*. OLFM4

◀ **Fig. 6 Streptococcal hydrogen peroxide inhibits gingipain activity and prevents *P. gingivalis*-induced Notch signaling. A** qRT-PCR of OLFM4 mRNA in TIGK cells left uninfected (NI) or challenged with *P. gingivalis* alone or in combination with *S. gordonii*, *S. oralis, S. sanguinis*, *S. constellatus*, or *S. mutans* for a total MOI of 100. **B** TIGK cells were grown in the lower chamber of a transwell plate and challenged with *P. gingivalis* (Pg) or left uninfected (NI). *S. gordonii* (Sg), *S. oralis* (So) or *S. mutans* (Sm) were added to the upper chamber where indicated, and OLFM4 mRNA was measured by qRT-PCR. **C** OLFM4 mRNA levels in TIGKs uninfected (NI), challenged with *P. gingivalis* (Pg), *S. gordonii* WT or *S. gordonii* mutant strains alone or together in equal numbers for a total MOI 100. **D** TIGK cells were grown in the lower chamber of a transwell plate and challenged with *P. gingivalis* (Pg) or left uninfected (NI). *S. gordonii* WT (Sg), *S. gordonii* SpxB mutant (ΔspxB), or complemented SpxB mutant (CΔspxB) were added to the upper chamber where indicated, and OLFM4 mRNA was measured by qRT-PCR. Data are means with SEM. $****P < 0.001$ compared to NI unless indicated. **E** *P. gingivalis* supernatant (PgS) was incubated with *S. gordonii* WT (Sg), SpxB mutant (ΔspxB), complemented SpxB mutant (CΔspxB) or *S. mutans* (Sm), cultured aerobically or anaerobically. Activity of RgpA/B was measured through cleavage of L-BAPNA chromogenic substrate. Data are means with SD and representative of three biological replicates. $*p < 0.05$, compared to PgS unless indicated. **F** *P. gingivalis* culture supernatant was reacted with the indicated concentrations of H_2O_2, and activity of RgpA/B was measured through cleavage of L-BAPNA chromogenic substrate. Data are means with SD and representative of three biological replicates. $*p < 0.05$, compared to *P. gingivalis* supernatant alone (0).

is a prosurvival glycoprotein which is overexpressed in human tumors, particularly those of the digestive system [48]. OLFM4 is also expressed in cells of the immune system and in inflammatory colonic epithelium [42, 49]. OLFM4 has relevance in the oral cavity, as it accumulates in the secretome of head and neck squamous cell carcinomas (HNSCCs), and is a potential biomarker for the disease [50]. Mechanistically, OLFM4 is involved in the regulation of EMT and of cell cycle progression by favoring transition from the S to G(2)/M phase [51, 52]. In this study we show the importance of OLFM4 in *P. gingivalis*-induced proliferation and migration of gingival epithelial cells.

Transcriptional profiling and siRNA knockdown experiments indicated that the Notch1-Jag1 signaling cascade is the major pathway through which OLFM4 is regulated by *P. gingivalis*. Notch signaling is a conserved pathway that controls cell fate decisions and plays critical roles in eukaryotic development and tissue homeostasis. Notch signaling also plays nuanced oncogenic or tumor-suppressive roles in different cancers depending on the tissue and cellular context [53]. Recently, Al-Attar et al. [54] found that activation of Notch signaling in oral mucosal and gingival epithelial cells by *P. gingivalis* leads to increased production of the anti-microbial protein PLA2-IIA, to which *P. gingivalis* is resistant. *P. gingivalis* can also stimulate Notch-1 expression and increase proliferation in aortic smooth muscle cells [55]. While *P. gingivalis* LPS has been shown to activate Notch signaling in osteoblasts

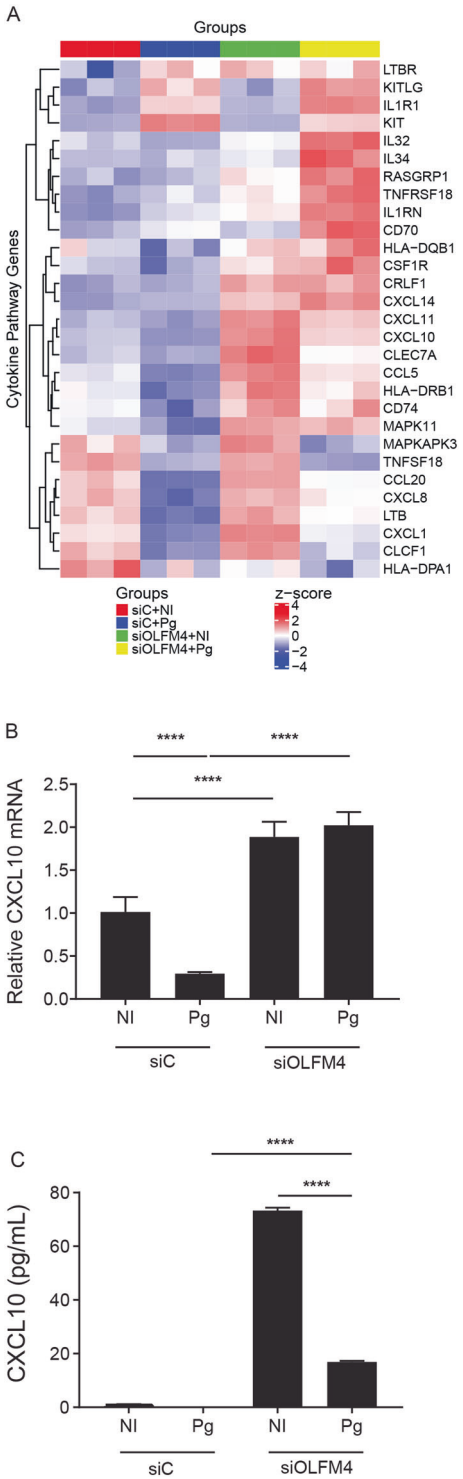

Fig. 7 OLFM4 regulates inflammatory responses to *P. gingivalis*. A Hierarchical clustering heatmap based on RNA-Seq log (RPKM) values of inflammatory genes differentially regulated in by challenge with *P. gingivalis* (Pg) in TIGKs transiently transfected with siRNA to OLFM4 or scrambled siRNA (siC). Color intensity denotes level of gene expression by z-score. **B** qRT-PCR of CXLCL10 transcripts and **C** ELISA of CXCLC10 protein in supernatants of TIGKs transiently transfected with siRNA to OLFM4 or scrambled siRNA (siC) and challenged with *P. gingivalis* (Pg) or left uninfected (NI). Data are means with SD and representative of 3 biological replicates. $****p < 0.001$.

[56], in epithelial cells the gingipain proteases are required for activation of Notch [54]. We have corroborated and extended these finding by showing that either the arginine-specific (RgpA/B) or lysine-specific (Kgp) enzymes can cleave and activate Notch1. Moreover, we established that the gingipains act on the extracellular domain of Notch1 and can functionally compensate for the loss or inhibition of host ADAM10/17 proteases. ADAM10/17 exert protease activity through a Zn^{2+}-dependent catalytic domain, and act on a wide range of membrane proteins resulting in ectodomain shedding [57]. Substrates for ADAM proteases include those involved in inflammation, apoptosis, cell adhesion, and cell proliferation [58]. ADAM10 expression is also associated with OSCC [59], and indeed ADAM10 and 17 have emerged as key therapeutic targets to inhibit the initiation and progression of a variety of tumors [60]. Further, we have reported previously that gingipain-dependent proteolysis at the membrane of TIGK cells causes ectodomain shedding, and the resulting sheddome contains a number of cell adhesion proteins [61]. Thus, overlapping ADAM/gingipain activity could represent an indirect means by which gingipains influence tumorigenic potential and inflammation. In addition to surface protein degradation, gingipains can activate signaling through Proteases Activated Receptors (PARs) [62, 63]. Triggering of PAR-3 by gingipains stimulates expression of the orphan chemokine CXCL14 (MIP2G). Interestingly, CXCL14 has bactericidal activity, to which *S. gordonii* is highly susceptible, while *P. gingivalis* is resistant [62]. This may represent a mechanism by which *P. gingivalis* can limit the antagonistic action of *S. gordonii* and is indicative of an interspecies 'arms race' based on long-standing evolutionary relationships between the organisms, as discussed further below.

In oral biofilm communities, *P. gingivalis* encounters a variety of other streptococci along with organisms more associated with periodontal destruction such as *T. denticola*, *F. nucleatum* and *F. alocis*. *P. gingivalis* is metabolically compatible with both *T. denticola* and *F. nucleatum*, and the organisms are synergistically pathogenic in animal models [37, 64–69]. *P. gingivalis* and *F. alocis* also show synergistic interactions in in vitro models of community formation and epithelial interactions [70–72]. In terms of regulation of OLFM4, *T. denticola*, *F. nucleatum* and *F. alocis* were unable to induce expression despite their proteolytic activity [73–76], although synergism with *P. gingivalis* was suggested from enhancement of *P. gingivalis* functionality in the dual species combinations. Nevertheless, direct OLFM4 regulation would appear to be a property restricted to *P. gingivalis* and its gingipains, reinforcing the concept that *P. gingivalis* has unique features that contribute to its success in the oral cavity and potential to contribute to disease.

The relationship between oral streptococci such as *S. gordonii* and *P. gingivalis* is dynamic and multitiered. At the epithelial surface *S. gordonii* can act as a homeostatic commensal and block transcriptional reprogramming by *P. gingivalis* [10]. In the current study we found that the underlying mechanism for *S. gordonii*-mediated antagonism of Notch signaling by *P. gingivalis* was inactivation of gingipains by hydrogen peroxide. Interestingly, H_2O_2 has been found to play a role in the interbacterial interactions of oral streptococci with other oral bacterial species including *Aggregatibacter actinomycetemcomitans* and *S. mutans* [38, 77–79]. As an anaerobe, *P. gingivalis* is susceptible to peroxide toxicity; however, the organism is capable of enduring exposure to H_2O_2 principally through the inherent catalase activity of bound ferrihemes [80]. Notably, H_2O_2 oxidizes hemoglobin to methemoglobin from which *P. gingivalis* can efficiently extract heme [81]. Hence, while we show that H_2O_2 can impede the action of gingipains on host cell signaling, any negative consequences for gingipain-dependent *P. gingivalis* metabolism may be offset by the availability of a readily extractable heme substrate.

S. gordonii and *P. gingivalis* display synergistic inflammatory periodontal tissue destruction [6, 8], a process in which OLFM4 may participate through modulation of immune signaling. In OLFM4 knockout mice, the production of proinflammatory cytokines and chemokines is increased following *H. pylori* infection [43]. Similarly, our RNA-Seq data showed that knockdown of OLFM4 caused an increase in the mRNA levels for several inflammatory mediators. With regard to periodontal destruction, therefore, upregulation of OLFM4 by *P. gingivalis* may prevent an effective antibacterial immune response, and contribute to the stealth-like properties of the organism [82]. Suppression of OLFM4 by *S. gordonii* would then contribute to a poorly controlled and destructive response which would initiate a burst of disease activity.

Bacteria colonizing surfaces of the oral cavity are organized into spatially constrained polymicrobial communities [35, 83]. In these social environments, organisms participate in multidimensional interactions which can be supportive or antagonistic, and, in general, eubiosis is maintained. However, a disruption of this intricate network can promote dysbiosis. Our current study would suggest that a relative decrease in the proportion of peroxide producing streptococci would relieve the suppression of gingipain activation of Notch signaling, increase the level of OLFM4 which in turn would promote epithelial cell proliferation and migration. While these are hallmarks of cancer, in vivo models would be required to establish any protective role of *S. gordonii* in tumor development, and indeed the role of *P. gingivalis* in the complex and dynamic oral microbial system. Conversely, an increase in the relative abundance of peroxide producing streptococci will inhibit the OLFM4

regulatory axis leading to destructive levels of inflammation in periodontal tissues. This prediction is supported by in vivo studies showing that *S. gordonii* and *P. gingivalis* are often found together in periodontal disease, and are physically associated in periodontal microbial communities [83, 84]. Identification of this H_2O_2-gingipain-OLFM4 signaling axis sheds new light on orally-relevant bacteria-bacteria and bacteria-host cell interactions.

Acknowledgements We thank the NIH/NIDCR for support through DE012505, DE023193, DE011111, DE017921 (RJL), DE028346 (DPM), DE028031, DE028296 (JB), and DE028166 (ZRF).

Compliance with ethical standards

Conflict of interest The authors declare no competing interests.

Publisher's note Springer Nature remains neutral with regard to jurisdictional claims in published maps and institutional affiliations.

References

1. Lamont RJ, Koo H, Hajishengallis G. The oral microbiota: dynamic communities and host interactions. Nat Rev Microbiol. 2018;16:745–59.
2. Fitzsimonds ZR, Rodriguez-Hernandez CJ, Bagaitkar J, Lamont RJ. From beyond the pale to the pale riders: The emerging association of bacteria with oral cancer. J Dent Res. 2020;99:604–12.
3. Al-Hebshi NN, Borgnakke WS, Johnson NW. The microbiome of oral squamous cell carcinomas: a functional perspective. Curr Oral Health Rep. 2019;6:145–60.
4. Hajishengallis G, Lamont RJ. Dancing with the stars: how choreographed bacterial interactions dictate nososymbiocity and give rise to keystone pathogens, accessory pathogens, and pathobionts. Trends Microbiol. 2016;24:477–89.
5. Jiao Y, Hasegawa M, Inohara N. The role of oral pathobionts in dysbiosis during periodontitis development. J Dent Res. 2014;93:539–46.
6. Daep CA, Novak EA, Lamont RJ, Demuth DR. Structural dissection and in vivo effectiveness of a peptide inhibitor of *Porphyromonas gingivalis* adherence to *Streptococcus gordonii*. Infect Immun. 2011;79:67–74.
7. Kuboniwa M, Houser JR, Hendrickson EL, Wang Q, Alghamdi SA, Sakanaka A, et al. Metabolic crosstalk regulates *Porphyromonas gingivalis* colonization and virulence during oral polymicrobial infection. Nat Microbiol. 2017;2:1493–9.
8. Mahmoud MY, Steinbach-Rankins JM, Demuth DR. Functional assessment of peptide-modified PLGA nanoparticles against oral biofilms in a murine model of periodontitis. J Control Release. 2019;297:3–13.
9. Mans JJ, von Lackum K, Dorsey C, Willis S, Wallet SM, Baker HV, et al. The degree of microbiome complexity influences the epithelial response to infection. BMC Genomics. 2009;10:380.
10. Ohshima J, Wang Q, Fitzsimonds ZR, Miller DP, Sztukowska MN, Jung YJ, et al. *Streptococcus gordonii* programs epithelial cells to resist Zeb2 induction by *Porphyromonas gingivalis*. Proc Natl Acad Sci USA. 2019;116:8544–53.
11. Miller DP, Fitzsimonds ZR, Lamont RJ. Metabolic signaling and spatial interactions in the oral polymicrobial community. J Dent Res. 2019;98:1308–14.
12. Lamont RJ, Hajishengallis G. Polymicrobial synergy and dysbiosis in inflammatory disease. Trends Mol Med. 2015;21:172–83.
13. Benjamini Y, Drai D, Elmer G, Kafkafi N, Golani I. Controlling the false discovery rate in behavior genetics research. Behav Brain Res. 2001;125:279–84.
14. Szklarczyk D, Gable AL, Lyon D, Junge A, Wyder S, Huerta-Cepas J, et al. String v11: Protein-protein association networks with increased coverage, supporting functional discovery in genome-wide experimental datasets. Nucleic Acids Res. 2019;47:D607–13.
15. Love MI, Huber W, Anders S. Moderated estimation of fold change and dispersion for RNA-Seq data with DESeq2. Genome Biol. 2014;15:550.
16. Team RCR: a language and environment for statistical computing. R Foundation for Statistical Computing 2019.
17. Tang Y, Horikoshi M, Li W. Ggfortify: Unified interface to visualize statistical results of popular R packages. R J. 2016;8:478–89.
18. Gu Z, Eils R, Schlesner M. Complex heatmaps reveal patterns and correlations in multidimensional genomic data. Bioinformatics. 2016;32:2847–9.
19. Lex A, Gehlenborg N, Strobelt H, Vuillemot R, Pfister H. Upset: Visualization of intersecting sets. IEEE Trans Vis Comput Graph. 2014;20:1983–92.
20. Liu W, Lee HW, Liu Y, Wang R, Rodgers GP. Olfactomedin 4 is a novel target gene of retinoic acids and 5-aza-2'-deoxycytidine involved in human myeloid leukemia cell growth, differentiation, and apoptosis. Blood. 2010;116:4938–47.
21. Liu W, Rodgers GP. Olfactomedin 4 expression and functions in innate immunity, inflammation, and cancer. Cancer Metastasis Rev. 2016;35:201–12.
22. Chen T, Siddiqui H, Olsen I. In silico comparison of 19 *Porphyromonas gingivalis* strains in genomics, phylogenetics, phylogenomics and functional genomics. Front Cell Infect Microbiol. 2017;7:28.
23. Dashper SG, Mitchell HL, Seers CA, Gladman SL, Seemann T, Bulach DM, et al. *Porphyromonas gingivalis* uses specific domain rearrangements and allelic exchange to generate diversity in surface virulence factors. Front Microbiol. 2017;8:48.
24. To TT, Liu Q, Watling M, Bumgarner RE, Darveau RP, McLean JS. Draft genome sequence of low-passage clinical isolate *Porphyromonas gingivalis* MP4-504. Genome Announc. 2016;4:e00256–16.
25. Acuna-Amador L, Primot A, Cadieu E, Roulet A, Barloy-Hubler F. Genomic repeats, misassembly and reannotation: a case study with long-read resequencing of *Porphyromonas gingivalis* reference strains. BMC Genom. 2018;19:54.
26. Ye L, Kriegl L, Reiter FP, Munker SM, Itzel T, Teufel A, et al. Prognostic significance and functional relevance of olfactomedin 4 in early-stage hepatocellular carcinoma. Clin Transl Gastroenterol. 2020;11:e00124.
27. Li Y, Gong Y, Ma J, Gong X. Overexpressed circ-RPL15 predicts poor survival and promotes the progression of gastric cancer via regulating mir-502-3p/OLFM4/STAT3 pathway. Biomed Pharmacother. 2020;127:110219.
28. Cong Z, Ye G, Bian Z, Yu M, Zhong M. Jagged-1 attenuates LPS-induced apoptosis and ROS in rat intestinal epithelial cells. Int J Clin Exp Pathol. 2018;11:3994–4003.
29. Ashizawa Y, Kuboki S, Nojima H, Yoshitomi H, Furukawa K, Takayashiki T, et al. OLFM4 enhances STAT3 activation and promotes tumor progression by inhibiting GRIM19 expression in human hepatocellular carcinoma. Hepatol Commun. 2019;3:954–70.
30. Lu J, Ye X, Fan F, Xia L, Bhattacharya R, Bellister S, et al. Endothelial cells promote the colorectal cancer stem cell

phenotype through a soluble form of Jagged-1. Cancer Cell. 2013;23:171–85.
31. Zhou Y, Sztukowska M, Wang Q, Inaba H, Potempa J, Scott DA, et al. Noncanonical activation of β-catenin by *Porphyromonas gingivalis*. Infect Immun. 2015;83:3195–203.
32. Lasica AM, Ksiazek M, Madej M, Potempa J. The type IX secretion system (T9SS): highlights and recent insights into its structure and function. Front Cell Infect Microbiol. 2017;7:215.
33. Bozkulak EC, Weinmaster G. Selective use of ADAM10 and ADAM17 in activation of Notch1 signaling. Mol Cell Biol. 2009;29:5679–95.
34. Mark Welch JL, Ramirez-Puebla ST, Borisy GG. Oral microbiome geography: micron-scale habitat and niche. Cell Host Microbe. 2020;28:160–8.
35. Mark Welch JL, Rossetti BJ, Rieken CW, Dewhirst FE, Borisy GG. Biogeography of a human oral microbiome at the micron scale. Proc Natl Acad Sci USA. 2016;113:E791–800.
36. Stacy A, McNally L, Darch SE, Brown SP, Whiteley M. The biogeography of polymicrobial infection. Nat Rev Microbiol. 2016;14:93–105.
37. Meuric V, Martin B, Guyodo H, Rouillon A, Tamanai-Shacoori Z, Barloy-Hubler F, et al. *Treponema denticola* improves adhesive capacities of *Porphyromonas gingivalis*. Mol Oral Microbiol. 2013;28:40–53.
38. Redanz S, Cheng X, Giacaman RA, Pfeifer CS, Merritt J, Kreth J. Live and let die: Hydrogen peroxide production by the commensal flora and its role in maintaining a symbiotic microbiome. Mol Oral Microbiol. 2018;33:337–52.
39. Kuboniwa M, Tribble GD, James CE, Kilic AO, Tao L, Herzberg MC, et al. *Streptococcus gordonii* utilizes several distinct gene functions to recruit *Porphyromonas gingivalis* into a mixed community. Mol Microbiol. 2006;60:121–39.
40. Potempa J, Nguyen KA. Purification and characterization of gingipains. Curr Protoc Protein Sci. 2007; 20:1–27.
41. Liu X, Ramsey MM, Chen X, Koley D, Whiteley M, Bard AJ. Real-time mapping of a hydrogen peroxide concentration profile across a polymicrobial bacterial biofilm using scanning electrochemical microscopy. Proc Natl Acad Sci USA. 2011;108:2668–73.
42. Shinozaki S, Nakamura T, Iimura M, Kato Y, Iizuka B, Kobayashi M, et al. Upregulation of Reg 1α and GW112 in the epithelium of inflamed colonic mucosa. Gut. 2001;48:623–9.
43. Liu W, Yan M, Liu Y, Wang R, Li C, Deng C, et al. Olfactomedin 4 down-regulates innate immunity against *Helicobacter pylori* infection. Proc Natl Acad Sci USA. 2010;107:11056–61.
44. Jauregui CE, Wang Q, Wright CJ, Takeuchi H, Uriarte SM, Lamont RJ. Suppression of T-cell chemokines by *Porphyromonas gingivalis*. Infect Immun. 2013;81:2288–95.
45. Takeuchi H, Hirano T, Whitmore SE, Morisaki I, Amano A, Lamont RJ. The serine phosphatase SerB of *Porphyromonas gingivalis* suppresses IL-8 production by dephosphorylation of NF-κB RelA/p65. PLoS Pathog. 2013;9:e1003326.
46. Bostanci N, Belibasakis GN. *Porphyromonas gingivalis*: an invasive and evasive opportunistic oral pathogen. FEMS Microbiol Lett. 2012;333:1–9.
47. Hajishengallis G. *Porphyromonas gingivalis*-host interactions: open war or intelligent guerilla tactics? Microbes Infect. 2009;11:637–45.
48. Zhang X, Huang Q, Yang Z, Li Y, Li CY. GW112, a novel antiapoptotic protein that promotes tumor growth. Cancer Res. 2004;64:2474–81.
49. Stark JE, Opoka AM, Fei L, Zang H, Davies SM, Wong HR, et al. Longitudinal characterization of olfactomedin-4 expressing neutrophils in pediatric patients undergoing bone marrow transplantation. PLoS One. 2020;15:e0233738.
50. Marimuthu A, Chavan S, Sathe G, Sahasrabuddhe NA, Srikanth SM, Renuse S, et al. Identification of head and neck squamous cell carcinoma biomarker candidates through proteomic analysis of cancer cell secretome. Biochim Biophys Acta. 2013;1834:2308–16.
51. Gao XZ, Wang GN, Zhao WG, Han J, Diao CY, Wang XH, et al. Blocking OLFM4/HIF-1α axis alleviates hypoxia-induced invasion, epithelial-mesenchymal transition, and chemotherapy resistance in non-small-cell lung cancer. J Cell Physiol. 2019;234:15035–43.
52. Kobayashi D, Koshida S, Moriai R, Tsuji N, Watanabe N. Olfactomedin 4 promotes S-phase transition in proliferation of pancreatic cancer cells. Cancer Sci. 2007;98:334–40.
53. Xiu MX, Liu YM, Kuang BH. The oncogenic role of Jagged1/Notch signaling in cancer. Biomed Pharmacother. 2020;129:110416.
54. Al-Attar A, Alimova Y, Kirakodu S, Kozal A, Novak MJ, Stromberg AJ, et al. Activation of Notch-1 in oral epithelial cells by *P. gingivalis* triggers the expression of the antimicrobial protein PLA2-IIA. Mucosal Immunol. 2018;11:1047–59.
55. Zhang B, Elmabsout AA, Khalaf H, Basic VT, Jayaprakash K, Kruse R, et al. The periodontal pathogen *Porphyromonas gingivalis* changes the gene expression in vascular smooth muscle cells involving the TGFβ/Notch signalling pathway and increased cell proliferation. BMC Genom. 2013;14:770.
56. Xing Q, Ye Q, Fan M, Zhou Y, Xu Q, Sandham A. *Porphyromonas gingivalis* lipopolysaccharide inhibits the osteoblastic differentiation of preosteoblasts by activating Notch1 signaling. J Cell Physiol. 2010;225:106–14.
57. Weber S, Saftig P. Ectodomain shedding and ADAMs in development. Development. 2012;139:3693–709.
58. Smith TM Jr, Tharakan A, Martin RK. Targeting ADAM10 in cancer and autoimmunity. Front Immunol. 2020;11:499.
59. Stasikowska-Kanicka O, Wagrowska-Danilewicz M, Kulicka P, Danilewicz M. Overexpression of ADAM10 in oral squamous cell carcinoma with metastases. Pol J Pathol. 2018;69:67–72.
60. Saha N, Robev D, Himanen JP, Nikolov DB. ADAM proteases: Emerging role and targeting of the non-catalytic domains. Cancer Lett. 2019;467:50–57.
61. Hocevar K, Vizovisek M, Wong A, Koziel J, Fonovic M, Potempa B, et al. Proteolysis of gingival keratinocyte cell surface proteins by gingipains secreted from *Porphyromonas gingivalis*—proteomic insights into mechanisms behind tissue damage in the diseased gingiva. Front Microbiol. 2020;11:722.
62. Aw J, Scholz GM, Huq NL, Huynh J, O'Brien-Simpson NM, Reynolds EC. Interplay between *Porphyromonas gingivalis* and EGF signalling in the regulation of CXCL14. Cell Microbiol. 2018;20:e12837.
63. Tada H, Matsuyama T, Nishioka T, Hagiwara M, Kiyoura Y, Shimauchi H, et al. *Porphyromonas gingivalis* gingipain-dependently enhances IL-33 production in human gingival epithelial cells. PLoS One. 2016;11:e0152794.
64. Kesavalu L, Holt SC, Ebersole JL. Virulence of a polymicrobic complex, *Treponema denticola* and *Porphyromonas gingivalis*, in a murine model. Oral Microbiol Immunol. 1998;13:373–7.
65. Ebersole JL, Feuille F, Kesavalu L, Holt SC. Host modulation of tissue destruction caused by periodontopathogens: effects on a mixed microbial infection composed of *Porphyromonas gingivalis* and *Fusobacterium nucleatum*. Micro Pathog. 1997;23:23–32.
66. Orth RK, O'Brien-Simpson NM, Dashper SG, Reynolds EC. Synergistic virulence of *Porphyromonas gingivalis* and *Treponema denticola* in a murine periodontitis model. Mol Oral Microbiol. 2011;26:229–40.
67. Bradshaw DJ, Marsh PD, Watson GK, Allison C. Role of *Fusobacterium nucleatum* and coaggregation in anaerobe survival in planktonic and biofilm oral microbial communities during aeration. Infect Immun. 1998;66:4729–32.
68. Tan KH, Seers CA, Dashper SG, Mitchell HL, Pyke JS, Meuric V, et al. *Porphyromonas gingivalis* and *Treponema denticola* exhibit metabolic symbioses. PLoS Pathog. 2014;10:e1003955.

69. Diaz PI, Zilm PS, Rogers AH. *Fusobacterium nucleatum* supports the growth of *Porphyromonas gingivalis* in oxygenated and carbon-dioxide-depleted environments. Microbiology. 2002;148:467–72.
70. Aruni AW, Roy F, Fletcher HM. *Filifactor alocis* has virulence attributes that can enhance its persistence under oxidative stress conditions and mediate invasion of epithelial cells by *Porphyromonas gingivalis*. Infect Immun. 2011;79:3872–86.
71. Aruni AW, Zhang K, Dou Y, Fletcher H. Proteome analysis of coinfection of epithelial cells with *Filifactor alocis* and *Porphyromonas gingivalis* shows modulation of pathogen and host regulatory pathways. Infect Immun. 2014;82:3261–74.
72. Wang Q, Wright CJ, Dingming H, Uriarte SM, Lamont RJ. Oral community interactions of *Filifactor alocis* in vitro. PLoS One. 2013;8:e76271.
73. Chioma O, Aruni AW, Milford TA, Fletcher HM. *Filifactor alocis* collagenase can modulate apoptosis of normal oral keratinocytes. Mol Oral Microbiol. 2017;32:166–77.
74. Ishihara K. Virulence factors of *Treponema denticola*. Periodontol 2000. 2010;54:117–35.
75. Aruni AW, Roy F, Sandberg L, Fletcher HM. Proteome variation among *Filifactor alocis* strains. Proteomics. 2012;12:3343–64.
76. Umana A, Sanders BE, Yoo CC, Casasanta MA, Udayasuryan B, Verbridge SS, et al. Utilizing whole fusobacterium genomes to identify, correct, and characterize potential virulence protein families. J Bacteriol. 2019;201:e00273–19.
77. Duan D, Scoffield JA, Zhou X, Wu H. Fine-tuned production of hydrogen peroxide promotes biofilm formation of *Streptococcus parasanguinis* by a pathogenic cohabitant *Aggregatibacter actinomycetemcomitans*. Environ Microbiol. 2016;18:4023–36.
78. Stacy A, Everett J, Jorth P, Trivedi U, Rumbaugh KP, Whiteley M. Bacterial fight-and-flight responses enhance virulence in a polymicrobial infection. Proc Natl Acad Sci USA. 2014;111:7819–24.
79. Stacy A, Fleming D, Lamont RJ, Rumbaugh KP, Whiteley M. A commensal bacterium promotes virulence of an opportunistic pathogen via cross-respiration. mBio 2016;7:e00782–16.
80. Smalley JW, Birss AJ, Withnall R, Silver J. Interactions of *Porphyromonas gingivalis* with oxyhaemoglobin and deoxyhaemoglobin. Biochem J. 2002;362:239–45.
81. Brown JL, Yates EA, Bielecki M, Olczak T, Smalley JW. Potential role for *Streptococcus gordonii*-derived hydrogen peroxide in heme acquisition by *Porphyromonas gingivalis*. Mol Oral Microbiol. 2018;33:322–35.
82. Hajishengallis G. Periodontitis: from microbial immune subversion to systemic inflammation. Nat Rev Immunol. 2015;15:30–44.
83. Valm AM, Mark Welch JL, Rieken CW, Hasegawa Y, Sogin ML, Oldenbourg R, et al. Systems-level analysis of microbial community organization through combinatorial labeling and spectral imaging. Proc Natl Acad Sci USA. 2011;108:4152–7.
84. Griffen AL, Beall CJ, Campbell JH, Firestone ND, Kumar PS, Yang ZK, et al. Distinct and complex bacterial profiles in human periodontitis and health revealed by 16S pyrosequencing. ISME J. 2012;6:1176–85.